The Functional Role of Positively Charged Amino Acid Side Chains in α-Bungarotoxin Revealed by Site-Directed Mutagenesis of a His-Tagged Recombinant α-Bungarotoxin†

Julie A. Rosenthal,‡ Mark M. Levandoski, Belle Chang, Jerald F. Potts, Qing-Luo Shi, and Edward Hawrot*

Department of Molecular Pharmacology, Physiology, and Biotechnology, Division of Biology and Medicine, Brown University, Providence, Rhode Island 02912

Received January 7, 1999; Revised Manuscript Received April 16, 1999

ABSTRACT: A polyhistidine tag was added to the N-terminus of α-bungarotoxin (Bgtx) recombinantly expressed in *E. coli.* The His-tagged Bgtx was identical to native, venom-derived Bgtx in its apparent affinity for the nicotinic acetylcholine receptor (nAChR) in *Torpedo* electric organ membranes. Furthermore, in a physiological assay involving mouse muscle nAChR expressed in *Xenopus* oocytes, the His-tagged Bgtx was as effective as authentic Bgtx at blocking acetylcholine-evoked currents. Ala-substitution mutagenesis of His-tagged Bgtx was used to evaluate the functional contribution of Arg36, a residue that is invariant among all α-neurotoxins. Replacement with Ala resulted in a 90-fold decrease in the apparent affinity for the *Torpedo* nAChR and a corresponding 150-fold increase in the IC_{50} for block of heterologously expressed mouse muscle nAChR, demonstrating the critical importance of this positive charge for the binding and functional activity of a long α-neurotoxin. The observed decrease in affinity corresponds to a $\Delta\Delta G$ of 2.7 kcal/mol and indicates that Arg36 makes a major contribution to complex formation. This finding is consistent with the proposal that Arg36 mimics the positive charge found on acetylcholine and directs the toxin to interact with receptor sites normally involved in acetylcholine recognition. In comparison, Ala-substitution of the highly conserved Lys26 resulted in only a 9-fold decrease in apparent affinity. Truncation of the His-tagged Bgtx following residue 67 produces a toxin lacking the seven C-terminal residues including the two positively charged residues Lys70 and Arg72. Truncation leads to a 7-fold decrease in apparent binding affinity.

The α-neurotoxins isolated from the venom of proteroglyphous (Elapid) snakes are extremely toxic due to their high affinity for the nicotinic acetylcholine receptor (nAChR)[1] found at the neuromuscular junction. These neurotoxins comprise a large family of sequence-related proteins that vary in length from 60 to 76 residues (for review, see ref *1*). These toxins are further subdivided into short and long neurotoxins with the short neurotoxins containing 60−62 amino acids and 4 conserved disulfide bridges. The long neurotoxins, with just a few exceptions, contain a characteristic fifth disulfide in addition to the four that are shared with the short neurotoxins and also feature several additional residues in the C-terminal region. Binding studies have suggested that the long neurotoxins bind more irreversibly than the short neurotoxins as demonstrated by the extremely slow rates of dissociation for the long neurotoxins (*1*). In addition, recent studies suggest that the long and short neurotoxins differ dramatically in their affinity for nAChRs composed of α7-subunits (*2*), further indicating that these two families of toxins may differ substantially in their mode of interaction with the various nAChRs.

α-Bungarotoxin (Bgtx), obtained from the venom of *Bungarus multicinctus*, is representative of the long neurotoxin family and because of its high affinity and specificity for nAChRs has provided a powerful tool for the biochemical and molecular study of this family of ligand-gated ion channels (*1*). A related but distinct long toxin found in the same venom, κ-bungarotoxin, in contrast to Bgtx, has low affinity for the muscle nAChR and instead recognizes certain neuronal forms of the nAChR in the peripheral and central nervous system (*3*−*5*). In addition, κ-bungarotoxin (also known as neuronal bungarotoxin) forms dimers under physiological conditions whereas the α-neurotoxins appear all to be monomeric (*3*, *4*). A number of the short and long neurotoxins have been isolated, and their structures have been determined through X-ray crystallographic studies and by solution NMR techniques (*6*−*8*). Initial attempts at exploring

† This research was supported by Research Grants NS34348 and GM32629 (to E.H.) from the National Institutes of Health. J.A.R. was supported in part by National Institutes of Health Predoctoral Training Grant GM07601 and her work was done in partial fulfillment of the requirements for a Ph.D. degree from Brown University.

* To whom correspondence should be addressed. Telephone: 401-863-1034. Fax: 401-863-1595. E-mail: Edward_Hawrot@brown.edu.

‡ Present address: Department of Cell Biology, Yale University School of Medicine, New Haven, CT.

[1] Abbreviations: nAChR, nicotinic acetylcholine receptor; Bgtx, α-bungarotoxin; BSA, bovine serum albumin; CD, circular dichroism; FPLC, fast protein liquid chromatography; H_7Bgtx, recombinant Bgtx encoded by vector pH_7BGTX containing a seven residue His tag appended to the N-terminus of the Bgtx coding sequence; IC_{50}, concentration resulting in a 50% reduction of the binding of radiolabeled authentic Bgtx to the nAChR or a 50% reduction in acetylcholine-evoked currents recorded from heterologously expressed nAChR; IPTG, isopropyl-β-D-thiogalactoside; LB, Luria−Bertani broth; PBS, phosphate-buffered saline; PCR, polymerase chain reaction; rBgtx, recombinant Bgtx; UV, ultraviolet.

10.1021/bi990045g CCC: $18.00
Published on Web 05/19/1999

the mechanism of receptor recognition by the toxins focused on chemical modification of toxin residues (*9*). More recently, recombinant expression systems have allowed the application of site-directed mutagenesis approaches to the determination of the structure−function relationship in this important group of toxins. Site-directed mutagenesis studies of the short neurotoxin erabutoxin *a* (*10*−*12*) have suggested important functional roles for both conserved and variant residues. The related short neurotoxin, Nmm I, has also been studied recently by site-directed mutagenesis (*13*). These latter studies suggest that certain mutant Nmm I toxins can discriminate between the two ligand binding sites on the mouse muscle nAChR. κ-Bungarotoxin's interaction with neuronal nAChRs, its weak binding to muscle nAChRs, and the structural role of individual disulfide bonds have also been investigated by site-directed mutagenesis (*5*, *14*, *15*).

We have previously described the recombinant expression in *E. coli* of the classic long neurotoxin Bgtx (*16*). We described the purification of the recombinant toxin (rBgtx), and we characterized the binding activity of the toxin containing the wild-type sequence in comparison to an Ala-substituted mutation at the highly conserved but not invariant Asp30 position (*16*). Our earlier studies demonstrated that neither the carboxyl side chain of Asp30 nor the N-terminus of Bgtx is directly involved in receptor recognition. In this study, we take advantage of our previous investigations of the functional role of the N-terminus in Bgtx to prepare an N-terminal His-tagged rBgtx with full receptor binding activity. We then use the minimally disruptive approach of Ala-substitution mutagenesis to investigate in a more quantitative fashion the contributions of the two highly conserved positively charged residues, Lys26 and Arg36, to binding and functional block. Further, we use deletion analysis to examine the functional and structural importance of the seven residues forming the C-terminal region of Bgtx.

EXPERIMENTAL PROCEDURES

Construction of a Recombinant Bgtx Synthetic Gene Containing a Histidine Tag. The sequences of the various oligonucleotide primers used for construction of the synthetic gene and for mutagenesis are available upon request. pBGTX1M3 (*16*) was used as a template for creating a new Bgtx fusion construct that contained the coding region for Gene-9, followed by a factor Xa protease recognition site (IEGR), a thrombin protease site (LVPR^{v}GS), and a seven amino acid histidine-tag, and ending with a synthetic gene for Bgtx. The mass of the expressed fusion protein was expected to be 43 kDa; of this, ∼9 kDa corresponds to H_7-Bgtx. Upon thrombin cleavage, the N-terminal sequence of the recombinant Bgtx is expected to be GSHHHHHHH. DNA containing this synthetic gene construct was amplified by PCR, and the purified product was digested with both *Hind*III and *Sal*I (Life Technologies, Inc.). The doubly digested 285 bp cassette was ligated into the pSR9 plasmid (Protein Polymer Technologies, Inc.). HB101 competent cells (Life Technologies, Inc.) were transformed with the ligation mixture, and single colonies were screened for inserts by PCR. Plasmid DNA was isolated from overnight cultures of one of the positive isolates, designated pH_7Bgtx-RQ, using Wizard mini-prep (Promega). The plasmid was used to transform cells of the expression strain BL21(DE3) (Novagen). The sequence was verified using Sequenase version 2.0 (USB).

Mutagenesis of pH_7Bgtx-RQ. pH_7Bgtx-RQ as well as pBGTX1M3, the template used for its construction, contain an Arg at position 71 and a Gln at position 72 based on the previously published sequence for Bgtx (*17*). The primary sequence for Bgtx has since been corrected to Gln71 and Arg72 (*18*). To make this change in the expression plasmid, pH_7Bgtx-RQ, we used the Transformer Site-Directed Mutagenesis kit (Clontech). The manufacturer's protocol was followed except that a second parental plasmid specific restriction digest was added to reduce parental colony background among transformants. Products from the mutagenesis were used to transform the expression strain BL21-(DE3) (Novagen). Plasmid DNA was isolated from a positive clone, designated pH_7Bgtx, and the sequence was confirmed.

Site-Specific Mutagenesis by Unique-Site Elimination. Using the Transformer kit (Clontech) as described above, three additional mutations were prepared in pH_7Bgtx: K26A, R36A, and Δ68−74, the deletion of residues His68 to Gly74. pH_7Bgtx was the template for the construction of pH_7Bgtx-K26A and pH_7Bgtx-R36A. The template for pH_7Bgtx-Δ68−74 was pH_7Bgtx-RQ. Products from the mutagenesis were used to transform chemically competent HB101 cells (Novagen). Plasmids from successful transformants were isolated (MiniPrep kit, Promega) and, after the sequences were confirmed, were used to transform the expression strain BL21(DE3) (Novagen).

Cell Growth Conditions for Expression of Bgtx Constructs. All constructs were grown in LB medium containing 100 μg/mL ampicillin (LB/amp). A single colony from a fresh agar plate was used to inoculate 250 mL of LB/amp medium, and the culture was grown at 37 °C until $A_{600} = \sim 0.3$. The overnight culture was added to 0.75 L of LB/amp in a Fernbach flask and grown at 37 °C at 300 rpm until the A_{600} was ∼0.7−0.8. Cultures were induced by the addition of IPTG to 0.5 mM and grown for 3 h. Cells were collected by centrifugation. The cell pellets were resuspended in 40 mL of "bind" buffer (0.5 M NaCl, 5 mM imidazole, and 20 mM Tris-HCl, pH 7.9) and either used immediately or frozen at −80 °C. Resuspensions (fresh or thawed) were passed through a French pressure cell (SLM Instruments) at 20 000 psi. The extract was clarified by centrifugation in a Ti60 rotor (Beckman) at 39 000 rpm at 4 °C for 20 min. The supernatant was filtered through a 0.8 μm filter prior to passage over a nickel affinity column. In some cases, a 2-L benchtop fermenter (Virtis) was used with appropriate scaling of media and reagents.

Nickel Affinity Chromatography. Soluble extracts prepared as described above were applied to a Ni^{2+} affinity column (Novagen) prepared according to the manufacturer's specification. Proteins were then sequentially eluted with 10 column volumes of "bind buffer" and with five column volumes of "wash" buffer (0.5 M NaCl, 20 mM Tris-HCl, pH 7.9, and 40 mM imidazole). Finally the fusion protein was eluted in 5 column volumes of elution buffer (0.5 M NaCl, 20 mM Tris-HCl, pH 7.9, 1 M imidazole).

Refolding. The nickel column eluant fraction containing the fusion protein was diluted to ∼1 mg/mL, and the correct disulfide pairs of the 10 cysteine residues of Bgtx were generated via a mixed-disulfide intermediate procedure as previously described (16). The refolded material was con-

centrated by stirred-cell ultrafiltration (Amicon) using a YM30 membrane. We attempted to cleave the fusion protein in solution but found that there were additional sites cleaved within the gene 9 sequence and that these fragments precipitate in the absence of the affinity resin.

Thrombin Cleavage. The refolded, concentrated histidine-tagged fusion protein in "bind" buffer was loaded onto the nickel affinity resin as described above. The resin was washed with 5 column volumes of 20 mM Tris, pH 8.2, 150 mM NaCl, and 2.5 mM $CaCl_2$, and additional cut buffer was then added to make the protein concentration ~1 mg/mL as estimated by the Bradford method. Thrombin (Boehringer Mannheim) was added to either 0.5% or 1% (w/w) and incubated with gentle agitation at room temperature. After 16−36 h of digestion, the resin was washed with 5 column volumes of "bind" buffer and 50 mL of elution buffer. Further buffer changes involved either dialysis against buffer A (50 mM sodium acetate, pH 5.2, 20 mM NaCl) or gel filtration with a PD10 desalting column (Pharmacia) equilibrated with buffer A.

Cation-Exchange Chromatography. Histidine-tagged toxins were loaded on a 1 mL prepacked Resource S column (Pharmacia LKB Biotechnology Inc.) in buffer A, and a wash with the same buffer removed unadsorbed material. The His-tagged toxins were eluted with a 35−55% gradient of 1 M NaCl in 50 mM NaOAc, pH 5.2. Peak fractions were desalted using PD10 gel filtration columns (Pharmacia) preequilibrated with 0.5% NH_4HCO_3, pH 7.5, or by dialysis against this same buffer using dialysis tubing with a cut off of 1000 daltons. Desalted samples were lyophilized and resuspended in an appropriate volume of 10 mM sodium phosphate buffer, pH 7.4, for binding assays. Bradford protein assays and SDS−PAGE analysis were done using standard methods.

^{125}I-Bgtx Solid-Phase Competition Binding Assay. The binding activity of recombinant toxin was determined in a competition binding assay using ^{125}I-labeled native Bgtx and acetylcholine receptor enriched membrane preparations as described previously (*16*). In the standard assay, *Torpedo* electric organ membranes (equivalent to 0.1 μg of protein) were plated into 96-well microtiter plates (Nunc, Immunosorb), resulting in 0.04 pmol of Bgtx binding sites adsorbed to the well as measured by saturation binding. The final concentration of ^{125}I-Bgtx used in the competition assays was 3 nM in an assay volume of 0.1 mL. The competition curves and resulting IC_{50} values from fitting the data were generated by using the dose−response (Logistic equation; mathematically analogous to the empirical Hill equation, ref *27*) curve-fitting program within Origin (Microcal). In the Logistic equation adapted to competition data, fractional binding of $^{125}\text{I-Bgtx} = 1/\{1 + ([\text{Bgtx}]/IC_{50})^n\}$. Identical IC_{50} values were obtained after 2 or 21 h of incubation as well as with decreased amounts of membranes added per assay well. The IC_{50} values obtained in such competition assays are directly related to the binding affinity of the mutant toxins for nAChR, and differences in IC_{50} values represent differences in the underlying affinities as described previously (*11*, *12*). The IC_{50} values reported here for wild-type and authentic Bgtx compare favorably to those previously reported for recombinant erabutoxin *a* which has an affinity comparable to that of Bgtx (*11*, *12*).

Electrophysiological Recordings from Oocyte-Expressed Acetylcholine Receptors. cRNAs, corresponding to the four mouse muscle AChR subunits, α, β, γ, and δ (plasmids provided by Jim Boulter), were prepared with an SP6 RNA polymerase kit (Megascript, Ambion Inc.). Chick α7 neuronal nAChR subunit cRNA was similarly prepared from a plasmid provided by M. Ballivet. Oocytes were injected with 15 ng of in vitro synthesized RNAs (3 ng each of β, γ, and δ, and 6 ng of α) in a total volume of 50 nL of H_2O using a Drummond nanojector. Oocytes were incubated in standard ND92 buffer at 19 °C for up to 6 days before recording.

Acetylcholine-evoked current responses were recorded using an OC-725b two-microelectrode voltage clamp (Warner Instruments, Hamden, CT) at room temperature 1−6 days after injection. Three 10 s pulses of 100 μM ACh were applied in control solution with 4 min washes of control solution between agonist applications. The three peak current amplitudes were averaged to determine the 100% agonist response. Responses were recorded and analyzed only for those oocytes in which the ACh-evoked responses were within the range that could be effectively voltage-clamped ($\leq$~10 μA). Oocytes were incubated in toxin solutions for 30 min, and the responses to 10 s pulses of 100 μM ACh were measured as described. The three post-Bgtx responses to ACh application were averaged. The block in ACh responses following toxin application was determined as the ratio of the post-Bgtx response to the control ACh response. Fractional block was plotted with Origin using the Logistic equation for dose−response curve-fitting.

RESULTS

In previous studies (*16*), we demonstrated that a recombinant Bgtx, encoded by the pBGTX1M3 expression vector, with 10 additional amino acid residues appended to the N-terminus of the coding sequence has an affinity for native nAChR that is virtually identical to native, venom-derived Bgtx. To make use of this evident tolerance of Bgtx for an N-terminal extension so as to facilitate purification of the recombinant toxin, we designed a new expression construct that incorporates an N-terminal polyhistidine tag. In addition, we introduced a thrombin cleavage site in the fusion protein at a position immediately N-terminal to the His-tag in order to release the H_7Bgtx from the expressed fusion protein.

Purification and Characterization of H_7Bgtx. The Gene9−H_7Bgtx fusion protein was overexpressed in *E. coli* upon induction with IPTG as previously described (*16*). SDS−PAGE analysis in conjunction with protein determinations revealed that the expressed H_7Bgtx fusion protein was found exclusively in the soluble fraction of the cell lysate, representing 15−22% of the total soluble protein (Figure 1A). The polyhistidine tag expedited purification of the H_7Bgtx fusion protein from the soluble cell lysate by selective interaction with a nickel-affinity resin. As shown in Figure 1A (lane 6), elution from this resin with 1 M imidazole resulted in a fraction greatly enriched in the fusion protein. At this stage in the purification, the H_7Bgtx fusion protein shows activity in a competition binding assay, confirming its identity as the overexpressed protein (Table 1).

The protein eluted with high imidazole was reduced with DTT and then treated with cystine as previously described (*16*) to generate the mixed disulfides which facilitate the correct formation of the five disulfides in Bgtx. We had previously shown that refolding at the fusion protein stage

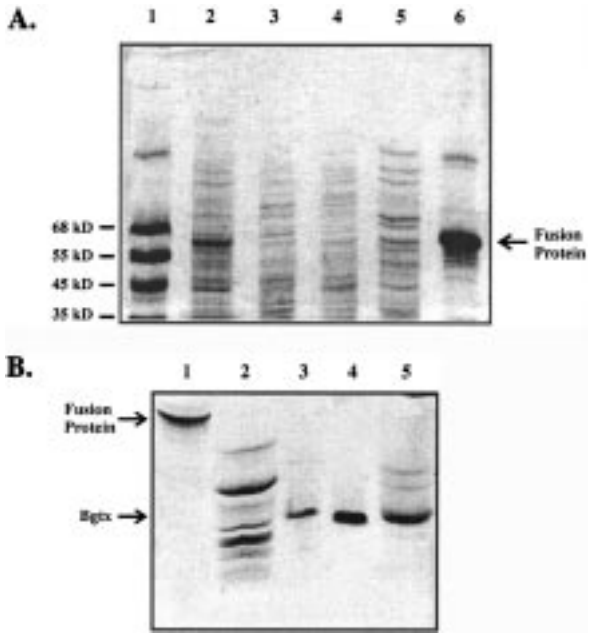

FIGURE 1: Isolation and purification of H_7Bgtx overexpressed in *E. coli*. (A) SDS−PAGE (7.5% polyacrylamide) gel of the H_7Bgtx fusion protein following purification with a nickel affinity column. Lane 1, protein molecular mass standards; lane 2, soluble fraction from IPTG induction prior to application onto the nickel column; lanes 3−5, sequential elution of the nickel column with 40 mM imidazole; and lane 6, protein eluted with 1 M imidazole. The position of H_7Bgtx fusion protein is marked by the arrow. (B) SDS−PAGE (20%) gel of H_7Bgtx at various stages of purification. Lane 1, H_7Bgtx fusion protein from lane 6 in panel A; lane 2, proteolytic fragments released from the nickel column upon digestion of the adsorbed H_7Bgtx fusion protein with thrombin; lane 3, protein eluted with 1 M imidazole; lane 4, authentic Bgtx; and lane 5, functionally active H_7Bgtx fraction following Resource S chromatography. In each case, 3 μg of protein was loaded per lane. Both gels were stained with Coomassie brilliant blue.

Table 1: Relative Binding Activity of Purified Fractions[a]

fraction	relative purity, [IC_{50} of purified Bgtx/ IC_{50} of fraction] × 100
1. fusion protein eluted from Ni^{2+} column	0.4
2. fusion protein after refolding	4.9
3. H_7Bgtx following thrombin cleavage and elution from Ni^{2+} column	18
4. H_7Bgtx after FPLC isolation	100

[a] IC_{50} values of H_7Bgtx were determined at various stages of purification, and the ratio of the IC_{50} of authentic Bgtx to these values was calculated. The molarity of protein used in the IC_{50} determination was based on the mass of the fusion protein in the first two fractions, and on the mass of H_7Bgtx in the final two purified fractions. The values presented are the averages from three separate purifications.

followed by proteolytic release of rBgtx was more efficient than the initial release of the rBgtx polypeptide from the fusion protein followed by its refolding (*16*). The "refolded" fusion protein showed an increase in specific binding activity as expected (Table 1). The fusion protein was subsequently reapplied to the nickel resin, and thrombin was added to the suspension to liberate H_7Bgtx from the fusion partner. Non-histidine-tagged cleavage products were washed from the resin while H_7Bgtx was eluted with 1 M imidazole (Figure 1B). SDS−PAGE analysis showed that the fractions selectively eluted from the nickel column with 1 M imidazole gave rise to a single band of protein that migrated at the

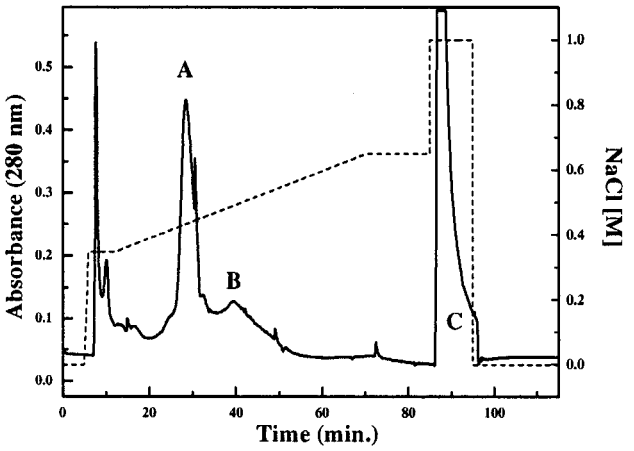

FIGURE 2: Resource S chromatography of H_7Bgtx. Protein (6.8 mg) eluted from a nickel affinity column following thrombin digestion was loaded onto a 1 mL Resource S cation-exchange column equilibrated in 50 mM sodium acetate, pH 5.2, containing 20 mM NaCl. Fractions were collected following elution with an increasing concentration of NaCl as indicated by the dotted line. The flow rate was 1 mL/min, and the absorbance of the eluted protein was monitored at 280 nm.

molecular mass (~9 kDa) expected for H_7Bgtx (Figure 1B, lane 3). Although this fraction appeared homogeneous by SDS−PAGE analysis, its specific activity (Table 1) suggested the presence of inactive protein. We further purified this fraction by cation-exchange chromatography (Resource S/FPLC) as shown in Figure 2. Three discrete peaks were observed upon salt gradient elution, all of which consisted primarily of a ~9 kDa protein (e.g., Figure 1B, lane 5). Rechromatography of the material isolated from each peak resulted in a single peak eluting at its original position. Peak "A" produced the highest specific activity in competition binding assays (Table 1 and see below). The total yield of protein from the peak "A" fraction ranged from 0.5 to 1.5 mg/L of initial culture medium.

The wild-type and all three mutant constructs expressed well in *E. coli* and resulted in similar amounts of refolded protein. The amounts of material eluted from the Resource S column were comparable in each case although the exact position of elution in the gradient varied somewhat with each mutant toxin as expected with a change in charge. In every case, the major peak of mutant toxin activity, as determined by the competition binding assay, corresponded with the major active fraction that eluted at ~0.4 M NaCl for the wild-type sequence (see below). Further evidence that the mutations produced little if any structural alterations was provided by circular dichroism (CD) spectroscopy (not shown). The secondary structure content for the recombinant wild-type and mutant toxins was calculated from the CD spectra by the method of Perczel et al. (*19*). The average values for β-sheet content were 28−31%, for α-helix 9−12%, for random coil 55−59%, and for β-turn 1−7%. Compared to venom-derived Bgtx, the random coil content of the His-tagged toxins is slightly elevated (~57% vs 38%) and the β-sheet content is slightly decreased (~30% vs 44%). These differences are most likely due to the significant spectroscopic contributions of the added polyhistidine sequence to the overall CD spectrum. Nonetheless, the mutant His-tag toxins show essentially the same secondary structure content as the His-tag wild-type toxin which has full activity.

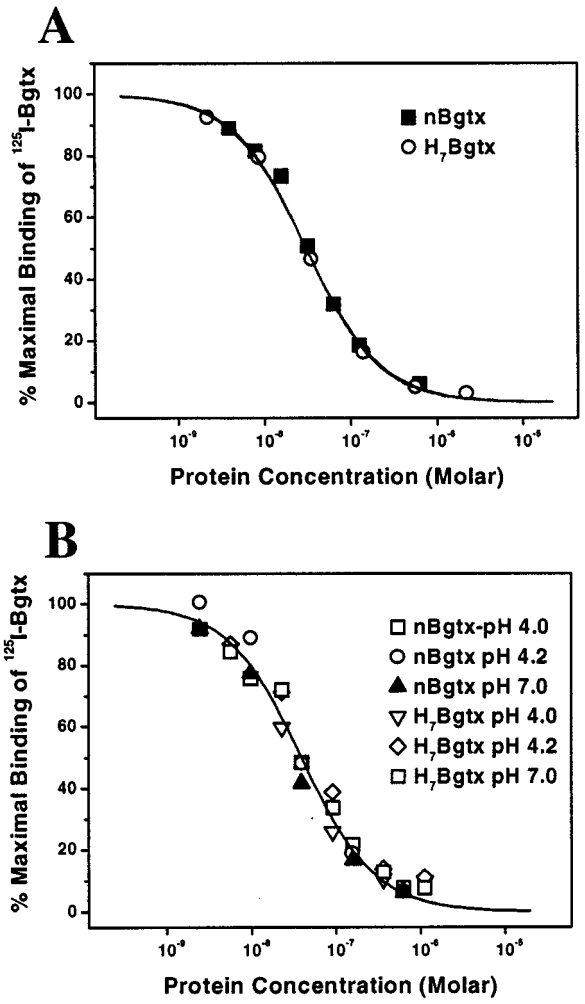

FIGURE 3: Solid-phase competition binding activity of H_7Bgtx. (A) Wells of microtiter plates were coated with 1 μg of *Torpedo* electric organ membranes and incubated with 3 nM ^{125}I-Bgtx and various concentrations of unlabeled venom-derived native Bgtx (nBgtx) or purified recombinant H_7Bgtx as described under Experimental Procedures. After a 2 h incubation, the wells were washed 4 times, and the bound radioactivity was determined. The values are averages of duplicate determinations. The competition curves were fit to the Logistic equation using the nonlinear curve-fitting routines in the commercial program Origin. (B) The pH dependence of binding to *Torpedo* membranes was determined for native and purified recombinant H_7Bgtx as described under Experimental Procedures. Values are averages of duplicate determinations.

Competition Binding Analysis. To follow the purification of H_7Bgtx and to determine the functional effects of various mutations, receptor binding activity was determined with solid-phase competition assays using ^{125}I-Bgtx and *Torpedo* electric organ membranes enriched in the nAChR (*16*). Under the standard assay conditions, a concentration of 35 nM venom-derived Bgtx produced a 50% decrease in the amount of ^{125}I-Bgtx bound to membranes after a 2 h incubation. The IC_{50} observed for the wild-type, authentic Bgtx is comparable to that reported for other α-neurotoxins that have been measured in similar competition experiments (*11*, *12*). As shown in Figure 3A and summarized in Table 1, an analysis of the protein fractions obtained by cation-exchange chromatography revealed that the activity (IC_{50} of 34 nM) of the material isolated in peak "A" (Figure 2) was identical to that of native, venom-derived Bgtx (IC_{50} of 35 nM). The material in peak "B" (Figure 2) migrated as a single ~9 kDa band on SDS gels, but its apparent affinity for the nAChR was decreased ~7-fold. Similarly, peak "C" also contained a single ~9 kDa protein band as determined by SDS−PAGE, but the activity of this material was decreased by ~17-fold. Using nonreducing conditions for SDS−PAGE analysis, we found that ~80% of peak "C" was an aggregate of high molecular weight complexes (data not shown). Attempts to refold the H_7Bgtx present in this fraction were unsuccessful. The final yields of recombinant Bgtx represent a 10−40% improvement over a recombinant Bgtx lacking the His-tag (*16*).

Side-by-side competition binding studies with the expressed rBgtx containing the wild-type sequence Gln71 and Arg72, produced by pH_7Bgtx, or that containing Arg71 and Gln72, produced by pBGTX1M3 (*16*), showed that the apparent binding affinities of these two recombinant toxins were identical to that obtained with native Bgtx (not shown). Thus, the reversal of the positions of these two residues in Bgtx has no effect on binding affinity.

Both at pH 7 and at pH 4 the Activity of H_7Bgtx Is Identical to Authentic Bgtx. To determine if the seven amino acid His-tag on H_7Bgtx affected receptor binding at low pH where the histidines would likely be positively charged, we performed a competition binding experiment at three different pH values with both native and H_7Bgtx (Figure 3B). The activity of H_7Bgtx at acidic pH values was identical to that obtained at neutral pH and in each case was identical to that of venom-derived Bgtx.

Site-Directed Mutagenesis of H_7Bgtx. The alanine-substituted toxins H_7Bgtx-K26A and H_7Bgtx-R36A were purified as described for wild-type toxin; each eluted from the Resource S column at essentially the same position as the wild-type H_7Bgtx (data not shown). A third mutated toxin, H_7Bgtx-Δ68−74, when analyzed by SDS−PAGE, migrated at approximately the same position as native toxin (~8 kDa; data not shown) as expected for a His-tagged toxin lacking seven C-terminal residues. The functional consequences of mutations introduced into H_7Bgtx by site-directed mutagenesis were tested using the competition binding assay. Representative binding curves obtained with each of the mutated toxins are displayed in Figures 4 and 5. In comparing the mean IC_{50} values from a minimum of three independent trials, we calculated apparent IC_{50} values of 35 ± 10 nM (±SEM) for native Bgtx and 34 ± 3 nM for H_7Bgtx. In contrast, the three mutated toxins showed a range of reduced binding affinities as revealed by corresponding increases in their IC_{50} values: H_7Bgtx-Δ68−74 (229 ± 47 nM) < H_7-Bgtx-K26A (310 ± 34 nM) < H_7Bgtx-R36A (3.1 ± 0.7 μM). In each binding assay, the fold-increase in IC_{50}, reflecting the fold-decrease in affinity for the mutated toxins, was calculated in comparison to wild-type Bgtx assayed at the same time. From this analysis, the average fold-decreases in binding affinity from the wild-type were 7-fold for H_7-Bgtx-Δ68−74, 9-fold for H_7Bgtx-K26A, and 90-fold for H_7-Bgtx-R36A.

Functional Blockade of Heterologously Expressed Mouse Muscle nAChRs. To provide an independent means of assessing the biological activity of H_7Bgtx and the mutated derivatives, we measured the ability of the various toxins to block ACh-evoked currents of mouse muscle nAChRs

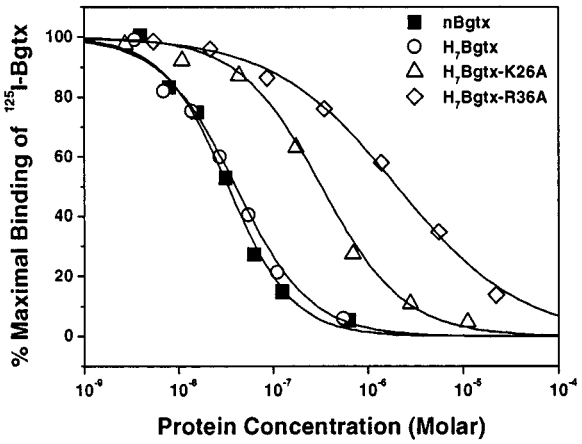

FIGURE 4: Solid-phase competition binding activity of H_7Bgtx-K26A and -R36A mutant toxins. The FPLC-purified mutant toxins were tested for binding competition to *Torpedo* membranes as described under Experimental Procedures. For internal comparison, the assay of native venom-derived Bgtx (nBgtx) was included in each binding experiment. Values are averages of duplicate determinations. The competition curves were fit to the Logistic equation using the nonlinear curve-fitting routines in the commercial program Origin.

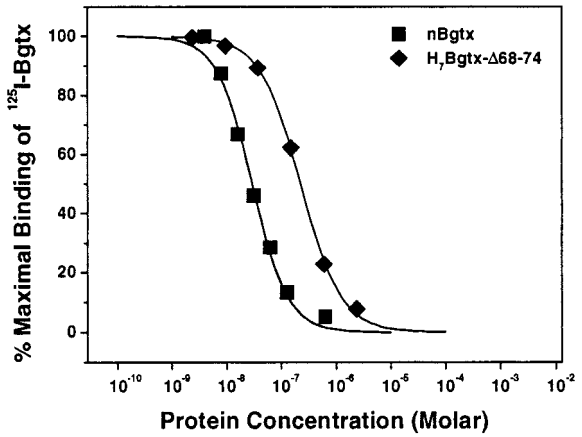

FIGURE 5: Solid-phase competition binding activity of the H_7Bgtx truncation mutant toxin lacking C-terminal residues 68−74. The FPLC-purified mutant toxin (H_7Bgtx-Δ68−74) and native Bgtx were tested for binding competition to *Torpedo* membranes as described in Figure 4.

heterologously expressed in *Xenopus* oocytes. This study also enabled us to investigate any species specificity to the effects of the toxin mutations. Each concentration of toxin was tested on at least three separate oocytes. The resulting dose−response curves for toxin block are shown in Figure 6. The apparent IC_{50} values observed in these assays were 2.2 nM for H_7Bgtx, 2.4 nM for Bgtx, 77 nM for H_7Bgtx-K26A, and 342 nM for H_7Bgtx-R36A. (Only one preparation of purified truncation mutant was tested in the oocyte assay; the results therefore, although generally consistent with the other mutant toxins tested, have not been included in the figure.) When compared to the activity of native Bgtx assayed under identical conditions, the mutated toxins had apparent affinities that were 2−4 times lower than expected from the solid-phase binding data utilizing *Torpedo* membranes. Nevertheless, the rank order of the mutated toxins based on functional blockade of oocyte-expressed mouse muscle nAChR was the same as that obtained in the competition binding assay (see Figures 4 and 5).

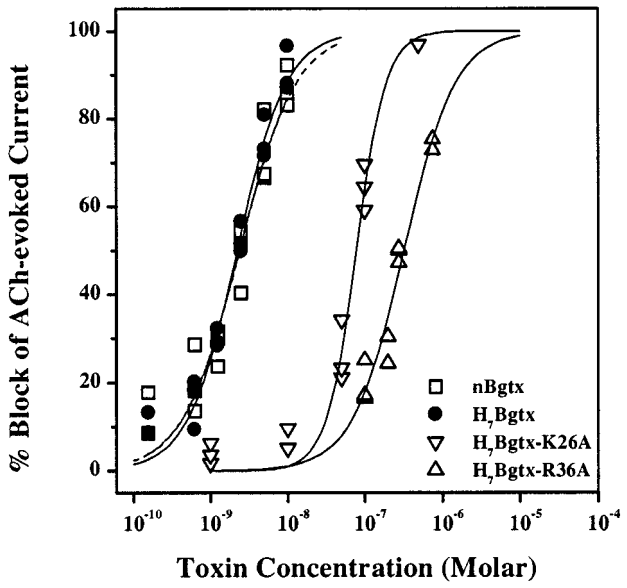

FIGURE 6: Acetylcholine-evoked currents blocked by H_7Bgtx mutant toxins in oocyte-expressed mouse muscle nAChRs. Mouse muscle nAChR subunit ($\alpha, \beta, \gamma, \delta$) cRNAs were injected into stage V *Xenopus* oocytes. Two-electrode voltage clamp recordings were made at −60 mV holding potential, and the peak current responses from three 10 s pulses of 100 μM ACh were averaged. Native (nBgtx) and H_7Bgtx mutant toxins were diluted into ND92 buffer containing 0.1 mg/mL BSA and perfused into the recording chamber for 2 min. The oocytes were incubated in the toxin solutions for 30 min, and the subsequent responses to three 10 s pulses of 100 μM ACh were averaged. The dose−response curves were generated using measurements from three different oocytes at each concentration of toxin.

DISCUSSION

We previously demonstrated that an extension of 10 amino acids on the N-terminus of Bgtx had little or no effect on binding activity (*16*). We subsequently prepared and characterized two additional constructs that effectively removed the factor Xa site and replaced it with either an enterokinase (DDDDK) or an acid-cleavable (DP) site (data not shown). Neither construct produced an active Bgtx of the molecular weight predicted for the cleavage site introduced at the N-terminus. These results suggest that the N-terminal Ile residue in Bgtx may have limited accessibility, a conclusion that is supported by the low reactivity of the N-terminal residues of Bgtx and cobratoxin to chemical modifying agents (*20*, *21*).

We demonstrate here that an N-terminal His-tagged Bgtx has full activity as measured either with a receptor binding assay utilizing *Torpedo* electric organ membranes (Figure 3) or with the functional blockade of heterologously expressed mouse muscle AChR (Figure 6). In addition, in preliminary studies with the homooligomeric chick α7 nAChR heterologously expressed in oocytes, H_7Bgtx was as effective as Bgtx in functional blockade of ACh-evoked currents (data not shown). The addition of the His-tag to the Bgtx sequence provides a convenient and facile means of protein isolation and purification. For these reasons, His-tagged Bgtx was used for the analysis of several mutations in Bgtx generated by site-directed mutagenesis. The availability of a fully functional His-tagged Bgtx significantly expands the repertoire of tools available for the study of toxin−receptor interaction and suggests that similar modi-

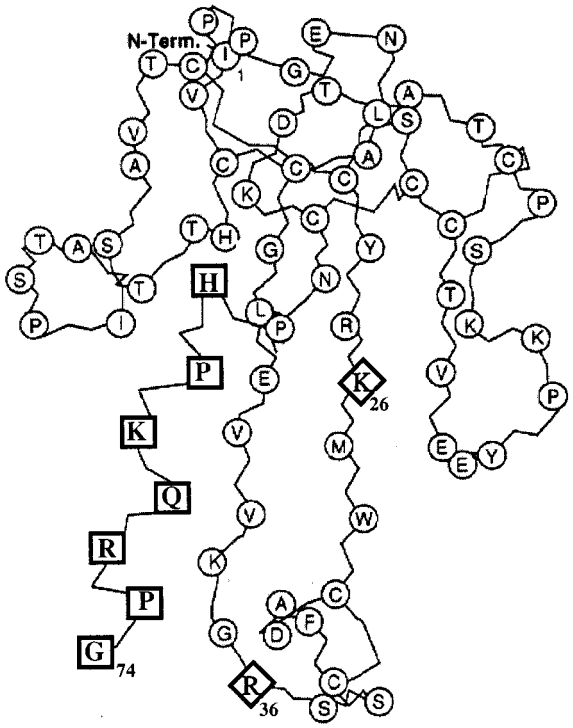

FIGURE 7: Schematic representation of the Bgtx residues studied in this report by Ala-substitution or deletion analysis. The positions of the 74 amino acids of Bgtx are shown as they would appear on the backbone structure of Bgtx determined by solution NMR (40). The invariant R36 and the highly conserved K26 are shown in boldface diamonds. Those residues outlined in boldface squares comprise the C-terminal tail region which characterizes the long α-neurotoxins.

fications could be successfully introduced into other members of the α-neurotoxin family.

The substitution of Ala residues for sites postulated to be involved in receptor−ligand interactions has been widely used to delineate the key residues at receptor−ligand interfaces (*22*, *23*). The effect of an Ala mutation is generally considered to be the simplest to interpret because this mutation is least likely to introduce new interactions either unfavorable or favorable. Changes in apparent binding affinities ($\Delta\Delta G$) can then be most directly interpreted as reflecting the contribution of the mutated residue to the free energy of binding. In the case of human growth hormone interaction with its receptor, a set of residues located on the periphery of the protein−protein contact zone produces no functional effect when mutated to Ala. These residues have been described as forming the "structural epitope" because they are indeed located at the contact zone but do not appear to contribute energetically to the protein−protein interaction (*23*−*25*). In contrast, residues comprising the "functional epitope" produce pronounced effects upon mutation to Ala. As few as 8 side chains in human growth hormone, out of the 31 side chains that are buried upon binding, contribute approximately 85% of the binding energy (*23*).

The Role of Lys26. Lys26 in Bgtx (Figure 7) corresponds to a highly conserved residue found in nearly all of the α-neurotoxins (1). The exceptional neurotoxins contain either a Met or a Glu residue at this position; for example, the Oh *a* toxin from *Ophiophagus hannah* contains a Glu in place of Lys and yet retains full toxicity in animal studies (*1*). Mutation of the corresponding Lys in erabutoxin *a* to a Glu resulted in a 175-fold decrease in the apparent binding affinity (*10*, *11*). Likewise, the replacement of this Lys in the related short α-neurotoxin Nmm I with a Glu led to a toxin with reduced affinity for the nAChR although in this case the mutation also produced differential effects on binding to the two subunit-specific binding sites on the nAChR (*13*). Whereas the native Nmm I toxin binds with equal affinity to the two neurotoxin binding sites (α/γ and α/δ) on the mouse muscle nAChR, the K27E mutation in Nmm I produced a toxin with a 13-fold reduction in apparent affinity for the α/δ site and a 390-fold reduction in apparent affinity for the α/γ site. Ala substitution at this site has not been previously investigated in either of the two short α-neurotoxins, erabutoxin *a* or Nmm I, nor in any other α- or κ-neurotoxin.

We find that the K26A mutation in Bgtx leads to a 9-fold decrease in the apparent binding affinity for the *Torpedo* nAChR (Figure 4) and a 34-fold decrease in affinity as measured by functional block of mouse receptors after 30 min of toxin incubation (Figure 6). The difference in the effectiveness of the K26A mutant in the two receptor assays may be related to the species difference between *Torpedo* and mouse nAChR. It is also possible that as the functional assay with oocytes was not performed under equilibrium conditions, there may be a significant difference in the rates of association between the mutant and wild-type Bgtx. In any case, the competition binding analysis of the K26A mutant Bgtx suggests that the side chain of Lys26 does indeed participate significantly in receptor binding, contributing about 1.3 kcal/mol (1 kcal = 4.18 kJ) to the binding interaction ($\Delta\Delta G = RT \ln [IC_{50}(\text{mutant})/IC_{50}(\text{wild-type})]$). The larger effects reported with the K27E mutation in erabutoxin *a* and Nmm I are presumably due primarily to the additional unfavorable interactions between the receptor and the mutant toxins because of the introduction of the carboxylate side chain into the toxin−receptor interface. There may also be fundamental differences in the mode of receptor interaction between Bgtx, a long α-neurotoxin, and erabutoxin *a* and Nmm I, two short α-neurotoxins. The long and short α-neurotoxins are known to differ substantially in the reversibility of their binding to the nAChR (*1*). Mutations in the nAChR have a more pronounced effect on the binding of Nmm I compared to Bgtx, further suggesting possible significant differences in binding modes between long and short α-neurotoxins (*26*).

We find no indication for differential binding of the K26A mutant Bgtx to the α/γ and α/δ receptor sites. Our competition data with the K26A mutant Bgtx are best fit by a simple Logistic equation with a pseudo-Hill coefficient (*27*) of 0.96 as shown in the representative binding competition curve (Figure 4). This value suggests that there is no discrimination between the two sites on the *Torpedo* nAChR.

The Role of Arg36. Substitution of Arg33 in erabutoxin *a* (which corresponds to Arg36 in Bgtx) with a Glu led to a greater than 318-fold decrease in the apparent binding affinity (*11*). Of the mutations studied, this effect on receptor binding was second in magnitude only to the S8T mutation (*12*). Replacement of Arg33 with Lys produced a 25-fold decrease (*11*) while substitution with the neutral but polar Gln side chain resulted in a 187-fold decrease in binding affinity (*12*). Our finding that Ala-substitution of the homologous Arg36 in Bgtx leads to a 90-fold decrease in the apparent binding

affinity ($\Delta\Delta G = 2.66$ kcal/mol) is most similar to the effect of the R33Q mutation in erabutoxin *a* and suggests that even the isosteric substitution with Gln may introduce new unfavorable side chain interactions. In any case, our results with Ala-substitution of the Arg side chain clearly demonstrate that Arg36 plays a critically important functional role in the long α-neurotoxins.

The difference in fold effects between the R36A (Bgtx) and R33Q (erabutoxin *a*) mutations may be due to the differential contribution of the conserved Arg to activity in the two toxins or may reflect the significant side chain differences between the Gln and Ala substitutions. The substitution of Ala for the homologous residue, Arg40, in κ-bungarotoxin, a neurotoxin related in sequence to the long α-neurotoxins, effectively abolishes the already quite low affinity ($IC_{50} = 10\ \mu M$) recognition of muscle receptors (*5*) and produces a greater than 100-fold decrease in the ability of the mutant toxin to block neuronal receptor activity as assessed in the chick ciliary ganglion system (*14*). The importance of Arg36 in several related neurotoxins is consistent with the proposed role of this residue as a mimic of the quaternary ammonium of acetylcholine (*9*). If this hypothesis is correct, then the cognate receptor residues interacting with Arg36 of Bgtx are likely to comprise a major determinant of the agonist binding site on the nAChR.

The two agonist binding sites in each nAChR molecule are believed to be located at the interface of the α/δ and α/γ subunits. It is clear that many small ligands bind at the two sites with different affinities, reflecting the different microenvironments at the two sites (*28*−*30*). In general, the short and long α-neurotoxins bind to the two sites with a single affinity suggesting that it is the α-subunit which provides the major determinants for toxin binding and/or that the contributions from the neighboring subunits are identical. A major role of the α-subunit in specifying Bgtx binding is supported by the observation that proteolytically derived fragments, synthetic peptides, and recombinantly expressed fragments corresponding to a short region on the α-subunit (*Torpedo*/mouse α-subunit residues 180−200) bind Bgtx with submicromolar affinity (*31*−*36*). Similar analyses of peptides or fragments derived from other regions and from other subunits of the receptor fail to reveal a consistent interaction of comparable affinity with Bgtx. Nevertheless, the γ and δ subunits may also contribute to or otherwise influence α-neurotoxin binding as suggested by recent mutational evidence (*13*, *26*, *37*).

Recombinant Nmm I neurotoxin binds with one affinity to the two sites present on the mouse nAChR. Of the two mutations, K27E and R33E, that reveal differential effects on binding to the two sites, the R33E mutation results in a larger reduction in the apparent binding affinity. There is a 680-fold decrease in affinity for the mouse α/δ site while binding to the neighboring α/γ site is decreased by 16 000-fold (*13*). Based on double mutant cycles involving charge reversal mutations, these two residues appear to interact with Val188 in the mouse α1 subunit (*26*) as well as other receptor residues in the vicinity of Val188. The substitution of an Ala for Arg36 in Bgtx (Figure 4) has a substantial and by far the largest effect that has been observed to date with any Bgtx mutation on the apparent binding affinity of the mutant toxin for the *Torpedo* nAChR. It is also the only mutation to date that may give a hint of nonequivalent binding sites for mutant toxins, as shown in the representative competition of Figure 4. In contrast to the K26A mutant where the pseudo-Hill coefficient (*27*) describing the slope of the curve is 0.96, as expected for simple competition with a single binding site, the pseudo-Hill coefficient obtained for the R36A mutation was significantly below that value (i.e., 0.67). In comparable analyses of Nmm I, a Hill coefficient for K27E and R36E of 0.6 was reported (*13*). The binding characteristics of the R36A mutant toxin may therefore suggest a differential effect of this mutation on the binding affinity for the two sites (α/γ and α/δ) on the nAChR. Further analyses involving other site-selective ligands would be needed, however, to quantitate the affinities of the two receptor sites for R36A Bgtx.

The C-Terminal Tail. The long- and short-chained α-neurotoxins vary in the amino acid sequence and length of the N-terminal toxin loop corresponding to residues 1−16 in Bgtx. They also differ dramatically in the length of the C-terminal tail region, which is 5−9 residues longer in the long-chained toxins (Figure 7). Our studies indicate that the removal of the seven carboxyl-terminal residues, HPKQRPG, which comprise ∼10% of the Bgtx sequence, results in a toxin with a ∼7-fold reduction in binding affinity ($\Delta\Delta G = 1.15$ kcal/mol) to the *Torpedo* nAChR. Previous work had shown that removal of the C-terminal 4−5 residues of Bgtx by carboxypeptidase P treatment resulted in a 15-fold reduction in Bgtx binding activity (*38*). Similarly, trypsin removal of two basic residues, Lys70 and Arg72, near the C-terminus resulted in a ∼15-fold reduction in binding activity (*39*). Our findings are generally consistent with these earlier results based on enzymatic treatment and suggest that the C-terminal seven residues contribute to receptor recognition to an extent that is approximately comparable to that of Lys26. What our studies further demonstrate is that the folding of Bgtx does not rely on an intact C-terminal tail in that the truncation mutant can be successfully and efficiently refolded in vitro.

NMR studies of the complex formed between Bgtx and a dodecapeptide (α185−196) from the α-subunit of the *Torpedo* nAChR revealed that the chemical shift positions of a number of protons in His68 were perturbed by greater than 0.15 ppm upon receptor peptide binding, suggesting that His68 may be in a position to be in close proximity to the receptor binding site (*40*). The apparent binding affinity of the truncation mutant toxin lacking the C-terminal residues beginning with His68, however, was no worse than the affinities reported for enzymatically treated Bgtx in which Lys70 and Arg72 were removed without apparent modification of His68. These results suggest that if His68 is at the contact zone between receptor and Bgtx, it is not likely to contribute much energetically to the interaction.

In conclusion, we have demonstrated that a His-tag addition to the N-terminus of Bgtx (Figure 7) has no adverse effect on toxin binding nor on its ability to block receptor function. The addition of a His-tag sequence to the N-terminus of Bgtx provides a convenient means for rapid isolation of the rBgtx from the expression system. In addition, we have demonstrated by means of Ala-substitution mutagenesis that the side chains of both Lys26 and Arg36 contribute significantly to the interaction of the long neurotoxin, Bgtx, with the *Torpedo* nAChR and with the mouse muscle nAChR. Analysis by Ala-substitution provides the

most meaningful estimate of the basic contribution of a toxin side chain to the binding energy. Residues Arg36 and Lys26 together with the C-terminal residues, 68−74, appear to contribute approximately 35% of the binding energy in the interaction of Bgtx and the *Torpedo* nAChR. This estimate assumes that the mutations studied here are independent in their functional effects and that no generalized structural alterations have been introduced. Additional studies of these and other Bgtx mutants may help elucidate the mechanisms underlying the essentially irreversible binding of Bgtx to the nAChR and the ability of the α-neurotoxins to interact with high affinity to nAChRs from a variety of vertebrate species.

REFERENCES

1. Endo, T., and Tamiya, N. (1991) in *Snake Toxins* (Harvey, A. L., Ed.) pp 165−222, Pergamon Press, New York.
2. Servent, D., Winckler-Dietrich, V., Hu, H. Y., Kessler, P., Drevet, P., Bertrand, D., and Ménez, A. (1997) *J. Biol. Chem. 272*, 24279−24286.
3. Loring, R. H., Chiappinelli, V. A., Zigmond, R. E., and Cohen, J. B. (1984) *Neuroscience 11*, 989−999.
4. Chiappinelli, V. A. (1993) in *Natural and Synthetic Neurotoxins* (Harvey, A., Ed.) pp 66−128, Academic Press, New York.
5. Fiordalisi, J. J., al-Rabiee, R., Chiappinelli, V. A., and Grant, G.A. (1994) *Biochemistry 33*, 12962−12967.
6. Low, B. W., Preston, H. S., Sato, A., Rosen, L. S., Searl, J. E., Rudko, A. D., and Richardson, J. S. (1976) *Proc. Natl. Acad. Sci. U.S.A. 73*, 2991−2994.
7. Walkinshaw, M. D., Saenger, W., and Maelicke, A. (1980) *Proc. Natl. Acad. Sci. U.S.A. 77*, 2400−2404.
8. Kosen, P. A., Finer-Moore, J., McCarthy, M. P., and Basus, V. J. (1988) *Biochemistry 27*, 2775−2781.
9. Karlsson, E. (1979) in *Snake Venoms, Handbook of Experimental Pharmacology* (Lee, C.-Y., Ed.) Vol. 52, pp 159−212, Springer-Verlag, Berlin.
10. Hervé, M., Pillet, L., Humbert, P., Trémeau, O., Ducancel, F., Hirth, C., and Ménez, A. (1992) *Eur. J. Biochem. 208*, 125−131.
11. Pillet, L., Tremeau, O., Ducancel, F., Drevet, P., Zinn, J. S., Pinkasfeld, S., Boulain, J. C., and Ménez, A. (1993) *J. Biol. Chem. 268*, 909−916.
12. Trémeau, O., Lemaire, C., Drevet, P., Pinkasfeld, S., Ducancel, F., Boulain, J. C., and Ménez, A. (1995) *J. Biol. Chem. 270*, 9362−9369.
13. Ackermann, E. J., and Taylor, P. (1997) *Biochemistry 36*, 12836−12844.
14. Fiordalisi, J. J., al-Rabiee, R., Chiappinelli, V. A., and Grant, G. A. (1994) *Biochemistry 33*, 3872−3877.
15. Grant, G. A., Luetje, C. W., Summers, R., and Xu, X. L. (1998) *Biochemistry 37*, 12166−12171.
16. Rosenthal, J. A., Hsu, S. H., Schneider, D., Gentile, L. N., Messier, N. J., Vaslet, C. A., and Hawrot, E. (1994) *J. Biol. Chem. 269*, 11178−11185.
17. Mebs, D., Narita, K., Iwanaga, S., Samejima, Y., and Lee, C. Y. (1971) *Biochem. Biophys. Res. Commun. 44*, 711−716.
18. Ohta, M., Ohta, K., Nishitani, H., and Hayashi, K. (1987) *FEBS Lett. 222*, 79−82.
19. Perczel, A., Park, K., and Fasman, G. D. (1992) *Anal. Biochem. 203*, 83−93.
20. Chang, C. C., Yang, C. C., Nakai, K., and Hayashi, K. (1971) *Biochim. Biophys. Acta 251*, 334−344.
21. Lin, S. R., and Chang, C. C. (1991) *Toxicon 29*, 937−950.
22. Cunningham, B. C., and Wells, J. A. (1989) *Science 244*, 1081−1085.
23. Cunningham, B. C., and Wells, J. A. (1993) *J. Mol. Biol. 234*, 554−563.
24. Dall'Acqua, W., Goldman, E. R., Lin, W., Teng, C., Tsuchiya, D., Li, H., Ysern, X., Braden, B. C., Li, Y., Smith-Gill, S. J., and Mariuzza, R. A. (1998) *Biochemistry 37*, 7981−7991.
25. Wells, J. A. (1996) *Proc. Natl. Acad. Sci. U.S.A. 93*, 1−6.
26. Ackermann, E. J., Ang, E. T. H., Kanter, J. R., Tsigelny, I., and Taylor, P. (1998) *J. Biol. Chem. 273*, 10958−10964.
27. Limbird, L. S. (1996) *Cell surface receptors: A short course on theory and methods*, 2nd ed., pp 105−106, Kluwer Academic Publishers, Dordrecht, The Netherlands.
28. Sine, S. M. (1993) *Proc. Natl. Acad. Sci. U.S.A. 90*, 9436−9440.
29. Kreienkamp, H.-J., Sine, S. M., Maeda, R. K., and Taylor, P. (1994) *J. Biol. Chem. 269*, 8108−8114.
30. Sine, S. M., Kreienkamp, H.-J., Bren, N., Maeda, R., and Taylor, P. (1995) *Neuron 15*, 205−211.
31. Wilson, P. T., Lentz, T. L., and Hawrot, E. (1985) *Proc. Natl. Acad. Sci. U.S.A. 82*, 8790−8794.
32. Gotti, C., Mazzola, G., Longhi, R., Fornasari, D., and Clementi, F. (1987) *Neurosci. Lett. 82*, 113−119.
33. Pearce, S. F., Preston-Hurlburt, P., and Hawrot, E. (1990) *Proc. R. Soc. London B, Biol. Sci. 241*, 207−213.
34. Fraenkel, Y., Navon, G., Aronheim, A., and Gershoni, J. M. (1990) *Biochemistry 29*, 2617−2622.
35. Conti-Tronconi, B. M., Diethelm, B. M., Wu, X., Tang, F., Bertazzon, T., Schroder, B., Reinhardt-Maelicke, S., and Maelicke, A. (1991) *Biochemistry 30*, 2575−2584.
36. Barchan, D., Kachalsky, S., Neumann, D., Vogel, Z., Ovadia, M., Kochva, E., and Fuchs, S. (1992) *Proc. Natl. Acad. Sci. U.S.A. 89*, 7717−7721.
37. Sine, S. M. (1997) *J. Biol. Chem. 272*, 23521−23527.
38. Endo, T., Oya, M., Tamiya, N., and Hayashi, K. (1987) *Biochemistry 26*, 4592−4598.
39. Wu, S.-H., Chen, C.-J., Tseng, M.-J., and Wang, K.-T. (1983) *Arch. Biochem. Biophys. 227*, 111−117.
40. Basus, V. J., Song, G., and Hawrot, E. (1993) *Biochemistry 32*, 12290−12298.

BI990045G